UDC 541.1:541.67

AGGREGATION MODES OF THE SPIN MONO-LABELED TYLOPEPTIN B AND HEPTAIBIN PEPTAIBIOTICS IN FROZEN SOLUTIONS OF WEAK POLARITY AS STUDIED BY PELDOR SPECTROSCOPY

A.D. Milov[1], Y.D. Tsvetkov[1], M. De Zotti[2], C. Prinzivalli[2], B. Biondi[2], F. Formaggio[2], C. Toniolo[2], M. Gobbo[2]

[1] *Institute of Chemical Kinetics and Combustion, Novosibirsk, 630090 Russian Federation,*
e-mail: tsvetkov@kinetics.nsc.ru
[2] *Institute of Biomolecular Chemistry, Padova Unit, CNR, Department of Chemistry, University of Padova, 35131 Padova, Italy*1.

The X-band PELDOR spectroscopy was used to investigate the magnetic dipole-dipole interactions in glassy solutions of nitroxide mono-labeled tylopeptin B and heptaibin peptaibiotics at 77 K. Specifically, a study was performed of the tylopeptin B peptides labeled at either position 3, 8 or 13, denoted as T3, T8 and T13, respectively. The heptaibin analogs labeled at either position 2 or 14, denoted as H2 and H14, respectively, were also investigated. It was shown that in frozen glassy peptide solutions in methanol, the spin labels are randomly distributed over the solvent volume. This result points to the absence of specific dipolar interactions between the peptides under these conditions. However, peptide aggregation was detected in weakly polar methanol/toluene environments. To study the properties of the resulting aggregates, we examined the depth of modulation for the PELDOR traces as a function of the concentration of the peptides in solution and the distances between the spin labels in the aggregates. Based on the concentration dependencies, the number of peptide molecules in the aggregates was estimated. We find that this value ranges from 2 to 3, depending on the position of the spin label in the peptide sequence. The combined analysis of the distance spectra and the number of peptide molecules in the aggregates allows us to suggest that dimer formation is the prevailing mode of self-association. In the case of spin-labeled tylopeptin B, the molecules in the dimer are head-to-head oriented. In addition, the distance spectra of the aggregates show that the C-termini of the molecules in the tylopeptin B dimer are more mobile than the N-termini. This phenomenon leads to an increase in the spread of the distances between the nitroxides as the label position is approaching the peptide C-terminus. For heptaibin, we show that two forms of dimerization (head-to-head and head-to-tail) occur. Finally, in addition to dimers, aggregates containing 3 or 4 peptide molecules, which give broad lines in the distance spectra, are seen in solution.

K e y w o r d s : PELDOR, dipole-dipole interactions, nitroxide mono-labeled tylopeptin B, heptabin, peptaibiotics.

INTRODUCTION

Information about the aggregation ability of peptides and the 3D-structure of their aggregates is an important factor to unravel the mechanism of action of many drugs and the steps leading to membrane pore formation. Here, pulsed electron-electron double resonance (PELDOR) spectroscopy, combined with site-directed spin labeling *via* chemical synthesis, was chosen as an effective methodology

to determine the structural parameters of peptides in different environments. The PELDOR technique allows one to measure both the distances between spins (in the 1.5—8 nm range) and the number of spin labels in the aggregates [1, 4].

The interaction between peptide antibiotics and phospholipid membranes is known to result in the formation of pores. This process takes place in a heterogeneous medium. As a rule, the diffusion of peptides to the hydrophilic membrane surface starts from an environment of fairly high polarity. However, the final peptide aggregate is identified in the hydrophobic part of the membrane, formed by the aliphatic tails of the phospholipids. The detailed mechanism for the formation of highly organized aggregates, upon transition of the peptides from a polar to an apolar medium is not yet completely clarified. In any case, information on the secondary and tertiary peptide structures in environments of various polarities is a major pre-requisite to establish how peptides permeate the biological membranes and to elucidate the mechanism of their action as antibiotics.

Peptide aggregation in both polar and apolar solvents has been investigated fairly deeply by methods of stationary (cw) and pulsed (PELDOR) EPR spectroscopy. In particular, the PELDOR technique has been already used both to study in detail the aggregation modes of the short peptaibiotic trichogin GA IV [5, 6] in frozen glassy matrices of various polarities and to extract data on the structures of its aggregates [7—9]. In refs. [10, 11], we applied the cw method of EPR spectroscopy to assess the formation of spin-labeled trichogin GA IV aggregates in solution. The aggregation process in polar matrices has been also investigated for the long peptaibiotics zervamicin [12, 13] and alamethicin [4, 14, 15].

In our ongoing program to study the properties of the peptaibiotic aggregates, in this work we analyzed the medium-length peptaibiotics tylopeptin B [16] and heptaibin [17]. Both compounds were spin mono-labeled at different positions of the peptide chain. The amino acid sequences of these peptaibiotic analogs (T3, T8, T13, H2, and H14) are illustrated in Scheme 1. These 14-amino acid peptides are characterized by a high content of the α-aminoisobutyric acid (Aib) residue (Scheme 1). Due to tetrasubstitution at its C^α-atom, Aib is responsible for the highly helical structure of the peptaibiotics [18] and, consequently, for their ability to permeate phospholipid bilayers. As spin label, we selected the equally helicogenic, nitroxide-containing, C^α-tetrasubstituted α-amino acid 4-amino-1-oxyl-2,2,6,6,-tetramethylpiperidine-4-carboxylic acid (TOAC) (Scheme 1) because: (i) it can appropriately replace Aib while maintaining the overall peptide 3D-structure and, most important for this study, (ii) its nitroxide moiety, tightly bound to the amino acid C^α atom, reflects directly any fluctuation of the peptide backbone. The conformations of native tylopeptin B and heptaibin have been already determined by CD and NMR in various solvents, including methanol [16, 17, 19]. Moreover, the PELDOR method has been used to study the 3D-structure of double spin-labeled tylopeptin B

Ac-Trp-Val-Aib-Aib-Ala-Gln-Ala-Aib-Ser-Aib-Ala-Leu-Aib-Gln-Lol   tyopeptin B
Ac-Trp-Val-**TOAC**[3]-Aib-Ala-Gln-Ala-Aib-Ser-Aib-Ala-Leu-Aib-Gln-Lol   T3
Ac-Trp-Val-Aib-Aib-Ala-Gln-Ala-**TOAC**[8]-Ser-Aib-Ala-Leu-Aib-Gln-Lol   T8
Ac-Trp-Val-Aib-Aib-Ala-Gln-Ala-Aib-Ser-Aib-Ala-Leu-**TOAC**[13]-Gln-Lol   T13

Ac-Phe-Aib-Aib-Aib-Val-Gly-Leu-Aib-Aib-Hyp-Gln-Aib-Hyp-Aib-Phol   heptabin
Ac-Phe-**TOAC**[2]-Aib-Aib-Val-Gly-Leu-Aib-Aib-Hyp-Gln-Aib-Hyp-Aib-Phol   H2
Ac-Phe-Aib-Aib-Val-Gly-Leu-Aib-Aib-Hyp-Gln-Aib-Hyp-**TOAC**[14]-Phol   H14
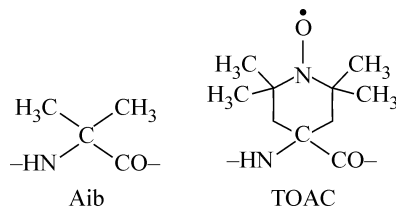
Scheme 1. Chemical structures of Aib and TOAC, and amino acid sequences of tylopeptin B and heptaibin and their TOAC mono-labeled analogs (Hyp, 4-hydroxyproline; Lol, leucinol; Phol, phenylalaninol)

and heptaibin analogs in methanol at 77 K [20]. The data obtained have shown that tylopeptin B has a typical α-helix structure, while heptaibin exists mostly in the 3_{10}-helix form. Finally, in such a polar solvent, these peptides do not aggregate [20].

In the PELDOR experiments, the spin system is subjected to the action of pulses at two different frequencies, ν_A and ν_B. The pulses at the detection frequency, ν_A, excite a portion of spins in the EPR spectrum (spins A) to generate a spin echo. The pulse at the pumping frequency, ν_B, excites another group of spins (spins B) and thus changes the sign of the dipole-dipole interaction between spins A and B. As a result, the amplitude of the spin echo signal (PELDOR signal) depends on the value of the dipole-dipole interaction between spins A and B, and on the position and intensity of the pumping pulse. This technique provides information on the parameters of the dipolar interaction between labels. Different pulse sequences have been proposed to perform PELDOR experiments. The most commonly used are the 3 (3P) [21] and 4 (4P) [22] pulse variants. In this work, we used the 3P PELDOR sequence.

MATERIALS AND METHODS

1. Peptide synthesis and characterization. Details of the syntheses and characterizations of tylopeptin B [16] heptaibin [17], and the three TOAC mono-labeled tylopeptin B analogs [19] have been recently published. Syntheses and characterizations of the two TOAC mono-labeled heptaibin analogs are described in the *Supporting Information*.

2. PELDOR and cw EPR experiments. For the PELDOR and cw EPR measurements, we dissolved the spin-labeled tylopeptin B (T3, T8 and T13) and heptaibin (H2 and H14) analogs in methanol or in a methanol/toluene mixture. In our experiments, methanol contained about 5 % ethanol as cryoprotector. The methanol to toluene ratio was 1:4 by weight for tylopeptin B and 1:9 for heptaibin. We used different compositions of methanol/toluene mixtures for the tylopeptin B and heptaibin analogs as these peptides have different abilities to form aggregates, depending on the solvent mixture composition. In both cases, we employed the optimal solvent mixture composition. A further increase in the toluene proportion reduces peptide solubility. All of the solvent mixtures allowed formation of a transparent glass by shock freezing of the sample in liquid nitrogen. The concentration of peptides was in a range from $3 \cdot 10^{-4}$ M to 10^{-2} M. A quartz ampoule of 0.4 cm in diameter containing 0.06 g of peptide solution was used.

The PELDOR data and the cw EPR spectra were obtained using an X-band Bruker ELEXSYS E580 EPR spectrometer. For the cw EPR measurements, the sample was placed in a finger of a quartz Dewar vessel, inserted into the spectrometer resonator. The cw EPR spectra were recorded at a modulation frequency of 100 KHz and a modulation amplitude of 0.1 mT. The microwave power level was set to a value low enough to avoid spectrum saturation. The PELDOR experiments were carried out using a dielectric Bruker ER 4118 X-MD-5 resonator and an Oxford Instruments CF-935 cryostat. The resonator was cooled with gaseous nitrogen. The sample temperature was kept near 77 K.

By analogy to ref. [20], in the 3P PELDOR sequence we used the pumping pulse scan which starts at time d_0 *before* the first detecting pulse. This methodology makes it possible to obtain the PELDOR signal value, V_0, when the pumping pulse passes an initial site of the scan from d_0 up to the first detecting pulse. The delay d_0 of the first detecting pulse relative to the beginning of the pumping pulse sweep amounted to 328 ns, thus allowing the pumping

Fig. 1. cw EPR spectra of frozen glassy solutions of the spin-labeled peptides studied. Curve *1*: T8 in methanol (Meth) (conc. $2.8 \cdot 10^{-4}$ M). Curves *2—4*: tylopeptin B analogs in the 1:4 w/w methanol/toluene (Tol) mixture (conc. for T8, T3, and T13: $6.2 \cdot 10^{-3}$ M, $8 \cdot 10^{-3}$ M, and $7.6 \cdot 10^{-3}$ M, respectively). Curves *5* and *6*: heptaibin analogs in the 1:9 w/w methanol/toluene mixture. (conc. for H2 and H14: $9 \cdot 10^{-3}$ M and $7 \cdot 10^{-3}$ M, respectively)
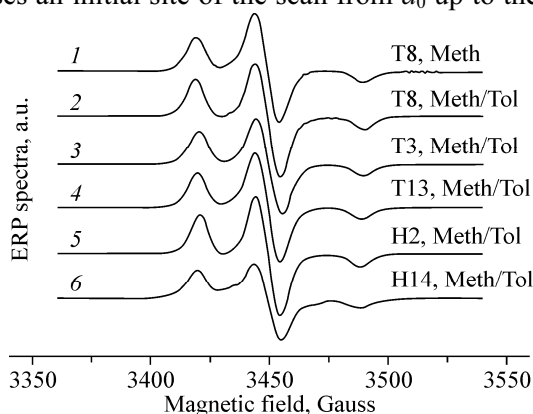
pulse to go through the first detecting pulse. All detecting pulses at the ν_A frequency are of equal intensity and of a 40 ns duration. The pumping pulse duration at the ν_B frequency was 36 ns. The turning angle of spins A under the detecting pulse action was maintained about 60° and was controlled using the echo signal shape and intensity. The rotation angle of spins B under the action of the pumping pulse was measured by comparison of the experimental and calculated shapes of the echo signal of spins A, provided that $\nu_A = \nu_B$. In this case, the pumping pulse was applied at the beginning of the scan ($d_0 = 328$ ns). The turning angle of spins B was 101±1°. In all of the experiments, the pumping pulse frequency was set at the maximum of the EPR spectrum. The probability for spin rotation by the pumping pulse, p_b, was calculated using relation (6) from ref. [21] and found equal to 0.154±0.002.

Usually, PELDOR experiments were conducted at $\nu_A = \nu_B + 60$ MHz. To inspect the orientation selectivity effects [23—28], the ($\nu_A - \nu_B$) value was varied from 40 to 90 MHz with steps of 10 MHz. The spin echo signal was integrated completely in a gate of 160 ns. The changes in the PELDOR signal upon passage of the pumping pulse through the detecting pulses were corrected by the method described in ref. [29]. The experimental approach to determine the beginning of the PELDOR trace analysis ($T = 0$) for the pumping pulse relative to the first detecting pulse is described in ref. [20].

RESULTS AND DISCUSSION

EPR spectra. Fig. 1 shows the cw EPR spectra of the frozen glassy solutions of the spin labeled peptides T3, T8 and T13 in the 1:4 *w/w* methanol/toluene mixture, and of the peptides H2 and H14 in the 1:9 *w/w* methanol/toluene mixture. The concentration of the peptides is $\approx 10^{-2}$ M. For comparison, Fig. 1 shows the spectrum of T8 in methanol. It can be seen that only the spectrum of H14 broadened as compared with those of the other peptides. The dipolar interactions between the labels do not contribute significantly to the EPR spectral shapes.

PELDOR DATA AND ANALYSIS

Aggregation of the mono-labeled peptides. Despite the absence of significant differences in the cw EPR spectra, the PELDOR time traces, $V(T)$, are quite different for peptide glassy frozen solutions in methanol and in the methanol/toluene mixtures. As an example, Fig. 2 shows the PELDOR time traces, $V(T)/V_0$, for T8 in glassy methanol at 77 K and different peptide concentrations. V_0 is the signal value in the absence of the pumping pulse. Here, the curves are linearly dependent on the delay time T. Similar linear dependencies are also seen for the peptides T3, T13, H2, and H14 in the same solvent.
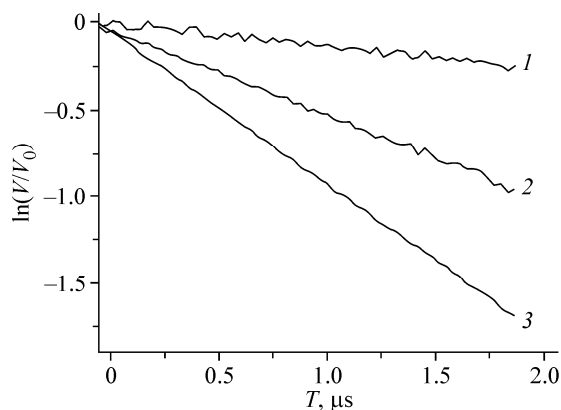

Fig. 2. PELDOR time T traces for T8 in frozen glassy methanol at 77 K. Curves *1*, *2*, and *3* are obtained at peptide concentrations $7.2 \cdot 10^{-4}$ M, $3.0 \cdot 10^{-3}$ M, and $6.2 \cdot 10^{-3}$ M, respectively
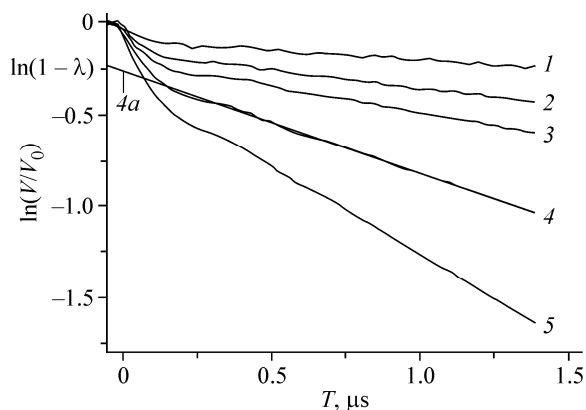
Fig. 3. PELDOR time T traces for T8 in a 1:4 w/w methanol/toluene mixture at 77 K. Curves *1*, *2*, *3*, *4*, and *5* refer to peptide concentrations $2.8 \cdot 10^{-4}$ M, $7.2 \cdot 10^{-4}$ M, $1.4 \cdot 10^{-3}$ M, $3.0 \cdot 10^{-3}$ M, and $6.2 \cdot 10^{-3}$ M, respectively. Curve 4a exemplifies how to remove the intermolecular contribution from curve 4 by smoothing oscillations by a second-order polynomial fit

According to the present-day accepted concepts [30, 31], a linear dependence of the PELDOR signal logarithm indicates a homogeneous, random distribution of the spin labels in the sample. In this case, the slope of the straight line, proportional to the concentration of T8, characterizes the efficiency of the *inter*molecular dipole-dipole interactions between the spin labels.

When a methanol/toluene mixture is used as a less polar environment, substantial changes in the PELDOR time traces take place. Fig. 3 shows the PELDOR time traces for the frozen glassy solutions of T8 in the 1:4 *w/w* methanol/toluene mixture at 77 K. As compared with the linear curves in Fig. 2 for the same peptide in methanol, the curves in Fig. 3 exhibit a fast decay in the PELDOR signal at short times ($T < 0.2$ μs), followed by a relatively slow decay, accompanied by oscillation dampings. Also, the modulation depth of the fast decay, λ, depends on peptide concentration. Similar concentration dependencies are observed for all of the peptides in this study.

The PELDOR time traces reported in Fig. 3 are typical of peptide aggregation [30]. The fast initial decay and the damping modulation are determined by the interaction between the spin labels in the aggregates. The slow decay of the signal at $T > 0.5$ μs is due to a weaker spin-label interaction between the aggregates. As a rule, these interactions are mutually independent. Therefore, the general signal decay, $V(T)$, can be represented as the product of the *intra*-aggregate, V_{INTRA}, and *inter*-aggregate, V_{INTER}, contributions as $V(T) = V_{INTRA}V_{INTER}$. The values of V_{INTRA} and V_{INTER} differ in their dependence on T. For $V_{INTRA}(T)$, typical is the fast decay in the range of the short T values, where T is either lower or of the same order of the inverse value of the dipolar interaction between the labels, with subsequent oscillations decaying with increasing T. $V_{INTER}(T)$ is a monotonous, almost exponential decay. The difference in the behaviors of V_{INTRA} and V_{INTER} *versus* T allows one to distinguish and to find them separately from the experimental overall $V(T)$ time traces. Curves 4 and 4a in Fig. 3 show the method for $V_{INTER}(T)$ and λ determinations. In particular, curve 4 denotes the experimental PELDOR time trace in the logarithmic form. Curve 4a smoothes the oscillations by the second-order polynomial fit. By moving curve 4a to the beginning of PELDOR decay, $\ln(V_{INTER}(T))$ is obtained. In this case, the value of the shift is $\ln(1 - λ)$, where the λ parameter indicates the modulation depth. Therefore, the *intra*-aggregate contribution $V_{INTRA}(T)$ is $\ln(V_{INTRA}(T)) = \ln(V(T)) - \ln(V_{INTER}(T))$.

Fig. 3 shows that an increase in peptide concentration, R_0, generates a higher modulation depth (λ), which testifies for a relative increase in fraction of the aggregated molecules. The $λ(R_0)$ data are reported in Fig. 4.

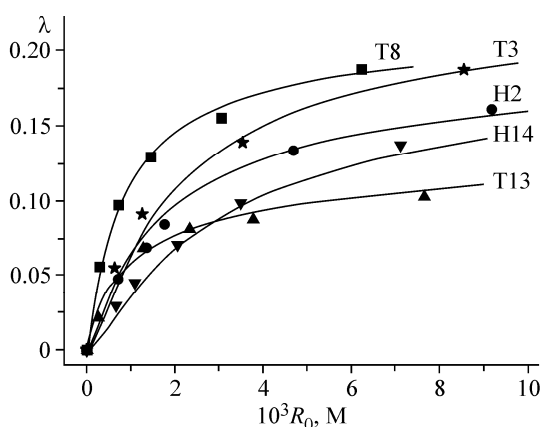*Fig. 4.* Dependencies of the modulation depth (λ) on concentration (R_0) of the five peptides studied. The symbols indicate experimental data. The solid lines were calculated using the parameters shown in Table 1
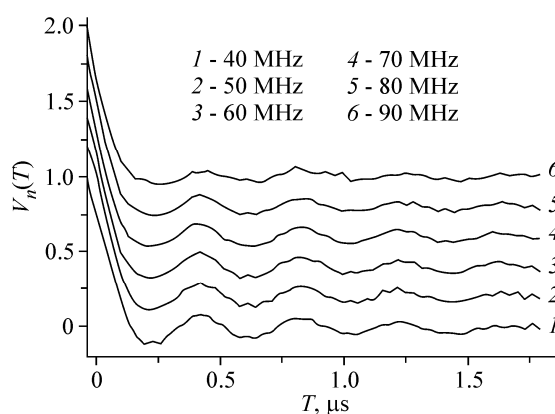
Fig. 5. Normalized *intra*molecular contribution to the PELDOR time traces for T3 in a 1:4 w/w methanol/toluene mixture at various values of $δν_{AB} = ν_A - ν_B$. The $δν_{AB}$ values are shown in the Figure. The peptide concentration is $1.5·10^{-3}$ M. For convenience, the curves are shifted relative to each other along the vertical axis by 0.2

Fig. 6. $V_n(T)$ time traces for the five mono-labeled peptides in methanol/toluene mixtures. Curve 1 is $\langle V_n(T)\rangle$ for T3 obtained by averaging of the dependencies shown in Fig. 5 (see text).The dotted lines denote experimental data. The solid lines were obtained using the distance distribution functions shown in Fig. 9. For convenience, the curves are shifted relative to each other
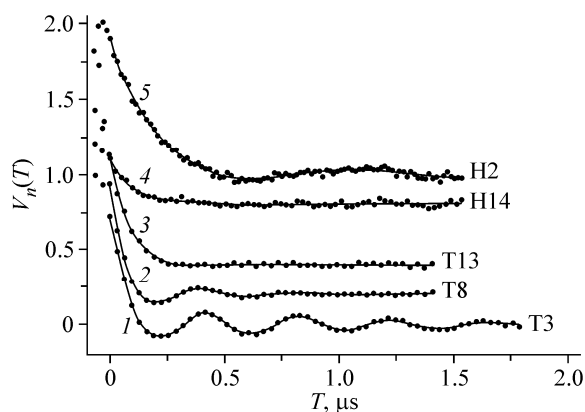
Figs. 5 and 6 describe the normalized *intra-*aggregate contribution, $V_n(T)$, obtained in accordance with [20] using the relation

$$V_n(T) = (V_{INTRA}(T) - V_{INTRA}(\infty))/$$
$$/(V_{INTRA}(0) - V_{INTRA}(\infty))$$

Here, $V_{INTRA}(\infty)$ is the asymptotic value of $V_{INTRA}(T)$ for long T and $V_{INTRA}(0)$ is the V_{INTRA} value in the absence of the pumping pulse.

Fig. 5 shows the orientation selectivity effect which was found for the peptide analog T3. The shape of $V_n(T)$ is a function of the difference $\delta\nu_{AB} = \nu_A - \nu_B$. In these measurements the pumping pulse frequency was kept constant and fixed at the integral EPR spectral maximum. Note that for all other peptides an orientation selectivity was not observed.

To solve the inverse problem of obtaining the distance spectrum from the $V_n(T)$ data, the orientation selectivity can be reduced by using the averaged PELDOR time trace $\langle V_n(T)\rangle$. For example, the T3 $\langle V_n(T)\rangle$ was obtained by summing up the PELDOR traces 1—6 in Fig. 5, each multiplied by the intensity of the normalized integral EPR line at a corresponding point ν_A ,as described in ref. [20]. Obtained in this way, the $V_n(T)$ dependence for T3 is given in Fig. 6. It should be mentioned that different methods of orientation selectivity averaging have been developed for the corrections of the distance distribution function [32—34].

Estimation of the number of peptide molecules in the aggregates from the PELDOR data. Presented in Fig 4, the experimental data on $\lambda(R_0)$ were analyzed on the assumption that an equilibrium between monomers and peptide aggregates does exist in a solution and the aggregates contain the same fixed number of peptide molecules.

Equilibrium analysis. If the solution contains both the monomers, *S*, and the aggregates, *C*, of spin-labeled peptide molecules, the spin echo signal in the PELDOR experiment is formed by a combination of those. In the simple case, when the aggregation can be described by an equilibrium between the peptide monomers and the aggregates containing *n* peptide molecules, the relation between the [*S*] and [*C*] concentrations is found from the kinetics relations:

$$n[S] \xleftrightarrow[k_2]{k_1} [C], \tag{1}$$

$$[S] + n[C] = [R_0], \tag{2}$$

$$[C] = K[S]^n. \tag{3}$$

Here, $[R_0]$ is the concentration of the peptide in solution and $K = \dfrac{k_1}{k_2}$ is the equilibrium constant of reaction (1). From relations (1)—(3) one can derive

$$[R_0] = \left(\frac{q}{(1-q)^n nK}\right)^{\frac{1}{n-1}}, \tag{4}$$

where

$$q = \frac{n[C]}{[R_0]}. \tag{5}$$

The last relations (4) and (5) establish a link between the ratio q, $[R_0]$, and K. Relation (4) can be given in a form convenient for analysis:

$$\ln(Q) = \ln([R_0]) + \frac{\ln(nK)}{n-1}, \tag{6}$$

where $Q = \left(\dfrac{q}{(1-q)^n}\right)^{\frac{1}{n-1}}$.

From the following analysis it turns out that the value of Q, expressed through the experimental PELDOR signal parameters, offers the possibility to determine the number of labels in the aggregate.

PELDOR *analysis in the presence of aggregates.* The PELDOR signal trace will depend on both the *inter*molecular interactions between spin labels and the peculiarities of the *intra*molecular interactions in the aggregates. Neglecting the possible distinctions between the *inter*molecular contributions from the monomers and aggregates, the PELDOR signal trace, $V(T)$, can be given as

$$V(T) = UV(T)_{INTER}([S] + n[C]V(T)_{INTRA}). \tag{7}$$

In this case, U is an instrumental constant, $V(T)_{INTER}$ is the contribution of the *inter*molecular interactions between spin labels to the PELDOR signal, and $V(T)_{INTRA}$ is the PELDOR time trace due to the interactions between labels in an aggregate. The values of $V(T)_{INTRA}$ and relation (7) are normalized to the concentration of the spin labels. In the absence of the *intra*aggregate interaction ($V(T)_{INTRA} = 1$) we have only *inter*molecular interaction and relation (7) has the form

$$V_0(T) = UV(T)_{INTER}([S] + n[C]) = UV(T)_{INTER}[R_0]. \tag{8}$$

The distinctive property of $V(T)_{INTRA}$ is its attenuation with increasing T, with possible oscillations due to dipole-dipole interactions between the labels inside the aggregate. According to ref. [30], for a sufficiently large T, when T is larger than the inverse of the characteristic dipole-dipole interactions of the labels inside the aggregate, the value of $V(T)_{INTRA}$ tends to its limiting value $V(\infty)_{INTRA}$. For the aggregate containing n spin labels, the limiting value of the PELDOR signal is given by

$$V(\infty)_{INTRA} = (1 - p_b)^{n-1}. \tag{9}$$

where p_b is the probability of the spin rotation by the pumping pulse.

Note that relation (9) has been verified experimentally on model compounds containing different number of spin labels [35, 36].

From relations (7)—(9) we can obtain:

$$\frac{V(\infty)}{V(0)} = \frac{[S] + n[C](1-p_b)^{n-1}}{[R_0]} = 1 - q(1-(1-p_b)^{n-1}) = 1 - \lambda. \tag{10}$$

Relation (10) between the magnitude of q and the experimental value $\lambda = 1 - V(\infty)/V(0)$ depends on the $[R_0]$ concentration. In addition, this relation connects q with p_b and n. As p_b is known from the experiment, the number of spins, n, can be determined using relations (6) and (10). With the help of (10), using the experimental values of λ and p_b, one can obtain the quantities q. By substituting the obtained q values in relation (6) and using the test n values ($n = 2, 3, 4$, etc.), we can plot $\ln(Q)$ as a function of $\ln[R_0]$. From all tested n values, we select an n for which $\ln(Q)$ is a linear function of $\ln[R_0]$ with a slope equal to 1. According to relation (6), the n value obtained in this way corresponds to the number of spin-labeled molecules in the aggregate. In addition, as $\ln(Q)$ at $\ln[R_0] = 0$ is equal to $\ln(nK)/(n-1)$, it is possible to estimate the equilibrium constant K.

As an example, Fig. 7 shows the dependence of $\ln(Q)$ on $\ln[R_0]$ for the peptide analog T8 for test values of n from 2 to 5. The Figure shows that the data are described by linear functions, with the slope angle α depending on the value of the chosen test n. An example of the slope angle as a function of n is shown in Fig. 8, which highlights that the condition $\tan(\alpha) = 1$ is satisfied when $n = 2.6 \pm 0.06$. A similar analysis was performed for all of the peptides. The n and $\ln(nK)/(n-1)$ values obtained are listed in Table. The calculated concentration dependencies of the modulation depth, $\lambda(R_0)$, using the data in Table, are reported in Fig. 4.

The data in Table show that, depending on the position of the label in the peptide, both the number of peptide molecules in the aggregate n and the value of the equilibrium constant K change. The n values are not integer values and are in the range from 2 to 3. These values (except for T13) contradict the original model of equilibrium between monomers and aggregates with the same fixed n.

PELDOR *data for the spin mono-labeled peptides studied* [a]

Peptide	n	$\dfrac{\ln(nK)}{n-1}$	Narrow line, r_{max}	Narrow line, Δ_{hh}	Broad line, r_{max}	Broad line, Δ_{hh}
T3	2,7±0,05	7±0,9	2,76	0,08	—	—
T8	2,6±0,06	7,3±1,1	2,7	0,2	—	—
T13	2±0,05	6,8±1,0	—	—	2,8	0,4
H2	2,4±0,1	6,8±1,5	2,7	0,12	3,75	0,25
H14	2,45±0,05	6,2±0,6	2,63	0,2	—	—

[a] n is the number of the spin-labeled molecules per aggregate;
K is the equilibrium constant between monomer and aggregates $(L/M)^{n-1}$;
r_{max} is the position of the line peak in the distance spectrum (nm);
Δ_{hh} is the half width at half height of the line in the distance spectrum (nm).
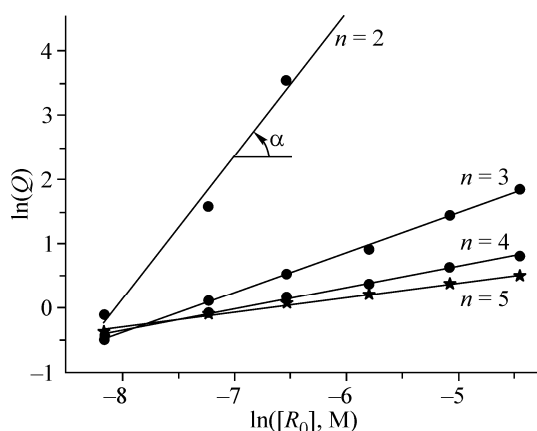

Fig. 7. An example of the logarithmic plot of the Q parameter as a function of peptide T8 concentration, $[R_0]$, in the 1:4 w/w methanol/ /toluene mixture at 77 K
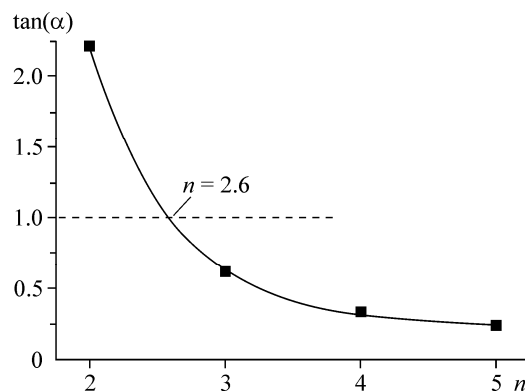

Fig. 8. Example of dependence of $\tan(\alpha)$ on the test n values. Points are taken from Fig. 7 and the solid line is its exponential fit

Apparently, there are aggregates in solution with various values of n, which are in equilibrium with each other and with the monomers. In this case, the experimental values of n should be considered as the average for all aggregates. This conclusion is confirmed by the distance spectra, $F(r)$, obtained for the spin labels in the tylopeptin B aggregates (see below).

Distance distribution between spin labels in aggregates. To obtain the spectra of the distances between the labels in the aggregates, we used the normalized dependence, $V_n(T)$, shown in Fig. 6. This method of analysis is given in detail in ref. [20] for the case of spin double-labeled peptides. The expression for $V_n(T)$ in the case of two spin dipoles interacting at a distance r, is given by

$$\int_{r_1}^{r_2} \tilde{F}(r)K(r,T)dr = V_n(T). \tag{11}$$

Here, $\tilde{F}(r)dr$ is proportional to the fraction of the spin pairs with the distance between the spins varying from r to $r + dr$ (r_1 and r_2 are the boundaries of the range of the r variations). The kernel of relation (11), $K(r, T)$, is obtained by Monte Carlo averaging of the core pair problem of ref. [20]. Relation (11) is a Fredholm integral equation of the first type. Its solution will afford the $\tilde{F}(r)$ function, which after normalization (the integral of it over r should be equal to unity), will allow one to calculate the desired distance distribution function $F(r)$ (distance spectrum).
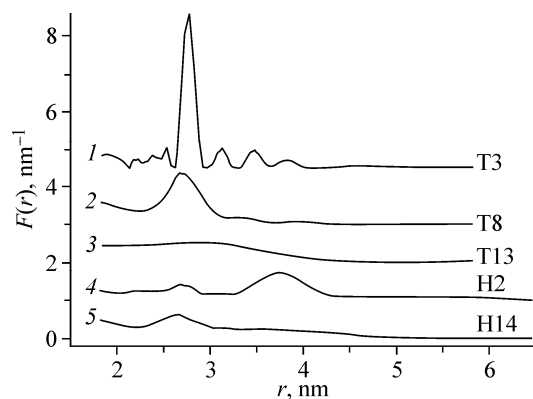
Fig. 9. Functions of distance distribution $F(r)$ between labels for the five peptides studied, obtained by solving the inverse problem based on the data in Fig. 6. For convenience, the curves are shifted relative to each other

The aggregates investigated in the present work usually contain more than two spins. In order to use the pair approximation for the $F(r)$ determination, the experimental conditions were chosen in such a way that the probability of excitation of spin A or spin B in a single aggregate would be rather small. In this case, essentially one spin A or B participates in the PELDOR signal formation. This condition makes it possible to use relation (11) to analyze the distance spectra between the spin labels in the aggregates.

Fig. 9 shows the resulting distance distribution functions $F(r)$ between the labels (distance spectra) in the aggregates of the mono-labeled peptides studied. The $F(r)$ functions were refined using the Tikhonov regularization method [37] by calculating the regularization parameters using the *L*-curve [38]. The distances obtained from the spectra maxima (r_{max}) and the widths at half height (Δ) of the lines are listed in Table 1. From Fig. 9 and Table 1, it is clear that all of the spectra contain lines with their maxima in the range of 2.6—4.5 nm.

Curves *1—3* in Fig. 9 refer to the spin-labeled tylopeptin B analogs. From these data, it follows that the change in the label position is accompanied by significant variations in the distance spectrum. It is for peptide T13 that the largest spread of distances is seen. On the other hand, for peptides T3 and T8 the spectra consist of a broad baseline and some narrow Gaussian-shaped lines, the fraction of which in the whole spectra is 0.6 and 0.42, respectively. The increase in the proportion of the narrow lines in the spectrum is accompanied by a modest increase of the *n* number from 2.6 to 2.7. Taken all of the results together, we conclude that at least two types of aggregates occur for tylopeptin B. The first type contains two molecules of the peptide, while the second is characterized by a higher number of molecules (for example, three).

For the tylopeptin B analog T3, the results are consistent with each other, if we assume that the narrow line (0.6 share part of the spectrum) belongs to the dimer with a rigid structure so that the phenomenon of orientation selectivity in the PELDOR time scans is observed (Fig. 5). Based on the average value of $n = 2.7$ (Table 1) and share 0.4 for the remaining part of the spectrum, we obtain $n = 3.8$ for this fraction of T3 peptide molecules in the aggregate. Considering that for peptide T8 the share part of the narrow dimer line is 0.42, we attribute the wide line of the spectrum to a trimer ($n=3$), which accounts for a 0.58 share part. For peptide T13, $n = 2$, that means that in solution only dimers with the widest measured range of distances between labels occur.

Thus, the general form of the aggregates of the tylopeptin B analogs is a dimer. The position of the maximum in the spectra of the distances in the dimers is almost independent of the site of the label in the peptide molecules. However, the spread of the distances increases significantly from T3 to T13. This finding leads to the qualitative conclusion that the molecules in the tylopeptin B dimers are head-to-head oriented. Moreover, the C-termini of the two molecules in the dimers are less close to each other than the N-termini. Clearly, this situation would lead to an increase in the spread of distances between the labels as the position of the label approaches the C-terminus.

The situation for the heptaibin analogs is more complicated. As in the case of the tylopeptin B analogs, the lines with a maximum near 2.6—2.7 nm can be assigned to dimers in which the molecules are head-to-head oriented. At the same time, for H2 we find a line with a maximum at the very long distance of 3.75 nm. We assign it to dimers with a head-to-tail type of orientation. As the H14 line at 3.75 nm is markedly broadened, the position of the label is expected to play a significant role on the flexibility of this type of dimers.

CONCLUSIONS

The cw EPR and PELDOR methods were used to study the magnetic dipolar interactions for solutions of the nitroxide spin mono-labeled tylopeptin B and heptaibin analogs at 77 K. Tylopeptin B analogs were labeled at position 3, 8 or 13. Heptaibin analogs were labeled at position 2 or 14.

We show that in methanol/toluene mixtures the spin labeled peptides form aggregates. The dependence of the degree of aggregation of peptides on the concentration of the peptide in solution was studied by PELDOR. Spectra of the distances between the spin labels in the aggregates were obtained.

Based on the analysis of the concentration dependence of the degree of peptide aggregation and the distance distribution spectra, we propose that the major form of the aggregate is a dimer. In the dimer, the spin-labeled tylopeptin B molecules are head-to-head oriented. Moreover, the C-terminal part of each tylopeptin B molecule is more mobile than its N-terminal part. This situation leads to a continuing increase in the spread of distances between the labels as the label moves closer to the C-terminus. Also, we find that there are two forms of heptaibin molecular orientation (head-to-head and head-to-tail) in the dimer. In addition to dimers, aggregates containing 3 or 4 peptide molecules occur, which are responsible for generation of the broad lines in the distance spectra.

SUPPORTING INFORMATION

Peptide synthesis and characterization. Fluorenylmethyloxycarbonyl(Fmoc)-amino acids were purchased from Novabiochem (Merck Biosciences, La Jolla, CA). All other amino acid derivatives and reagents for peptide synthesis were supplied from Sigma-Aldrich (St. Louis, MO), except for N-ethyl, N′-[3-(dimethylamino)propyl]carbodiimide (EDC), O-(7-azabenzotriazol-1-yl)-1,1,3,3-tetramethyluronium hexafluorophosphate (HATU) and 7-aza-1-hydroxy-benzotriazole (HOAt), which were purchased from GL Biochem (Shangai, China). Manual solid-phase peptide syntheses were performed on a 0.05 mmol scale, starting with the L-phenylalaninol-substituted 2-chlorotrityl resin (Iris Biotech, Marktredwitz, Germany) (125 mg, loading 0.40 mmol/g). The deprotection of the Fmoc group, performed with 20 % piperidine solution in N,N-dimethylformamide, was repeated twice. To avoid the formation of the 2,5-dioxopiperazine byproduct at the level of the free N-terminal -H-Aib-Hyp- dipeptide sequence, the Fmoc-protection was removed from Aib[12] and Aib[9] in two steps of five minutes each, instead of using the standard procedure which requires two steps of ten and fifteen minutes each. The coupling steps were carried out in the presence of HATU (HATU, N,N'diisopropylethylamine, 45 min coupling time, N,N-dimethylformamide as the solvent), except for the coupling of side-chain unprotected Fmoc-Gln-OH where HOAt was added to prevent the ε-nitrile formation. All coupling steps were doubled, except when Aib was not involved. The coupling steps were all conducted in the presence of an excess of 3 equiv. of the acylating agent, except when Fmoc-Hyp-OH was involved. In this latter case, a 0.5 equiv. excess was employed, to minimize the risk of self-acylation at the unprotected, γ-hydroxyl group. The final acetylation at the N-terminus was achieved using the preformed activated ester of acetic acid, obtained by reaction with an equivalent amount of EDC and HOAt, in the presence of N-methylmorpholine. The 1-hr coupling procedure was repeated twice. Cleavage of the peptide from the 2-chlorotrityl resin was performed by repeated treatments with 30 % 1,1,1,3,3,3-hexafluoroisopropanol in distilled CH_2Cl_2 (45 min each and overnight). The heptaibin analogs were purified by preparative RP-HPLC on a Phenomenex Jupiter C_{18} column (21.2×250 mm, 10 μ, 300 Å) using a Shimadzu (Kyoto, Japan) LC-8A pump system equipped with a SPD-6A UV-detector (flow rate 15 ml/min, spectrophotometric detection at λ = = 216 nm) and a binary elution system: A, H_2O; B, CH_3CN/H_2O (9:1 *v/v*); gradient 45 %—65 % B in 20 min [in the absence of trifluoroacetic acid, a cleaving agent for the Aib-Hyp bonds]. The purified fractions were characterized by analytical RP-HPLC on a Phenomenex Jupiter C_{18} column (4.6× ×250 mm, 5 μ, 300 Å) using an Agilent 1200 series HPLC (Agilent Technologies, Santa Clara, CA). The binary elution system used was: A, H_2O/CH_3CN (9:1 *v/v*); B, CH_3CN/H_2O (9:1 *v/v*); gradient 30 %—90 % B in 20 min (flow rate 1 ml/min); spectrophotometric detection at λ = 216 nm. Retention

times: [TOAC^2]-heptaibin (H2): 11.9 min; [TOAC^{14}]-heptaibin (H14): 12.3 min. Yield of purified [TOAC^2]-heptaibin (H2): 20 %. Yield of purified [TOAC^{14}]-heptaibin (H14): 15 %. Purity: >96 %.

Electrospray ionization (ESI-MS) was performed using a PerSeptive Biosystem Mariner instrument (Framingham, MA). [TOAC^2]-heptaibin (H2) (*m/z*): calculated for $C_{82}H_{128}N_{17}O_{20}$ [M+H]$^+$ 1672.96 found 1672.89. [TOAC^{14}]-heptaibin (H14) (*m/z*): calculated for $C_{82}H_{128}N_{17}O_{20}$ [M+H]$^+$ 1672.96; found 1673.02.

REFERENCES

1. *Tsvetkov Yu.D., Milov A.D., Maryasov A.G.* // Rus. Chem. Rev. – 2008. – **77**. – P. 487 – 520.
2. *Milov A.D., Samoilova R.I., Tsvetkov Yu.D., Formaggio F., Toniolo C., Raap J.* // J. Amer. Chem. Soc. – 2007. – **129**. – P. 9260 – 9261.
3. *Milov A.D., Tsvetkov Yu.D., Formaggio F., Oancea S., Toniolo C., Raap J.* // Phys. Chem. Chem. Phys. – 2004. – **6**. – P. 3596 – 3603.
4. *Milov A.D., Samoilova R.I., Tsvetkov Yu.D., Jost M., Peggion C., Formaggio F., Toniolo C., Handgraaf J.-W., Raap J.* // Chem. Biodivers. – 2007. – **4**. – P. 1275 – 1298.
5. *Toniolo C., Brückner H.* Peptaibiotics: Fungal Peptides Containing α-Dialkyl α-Amino Acids. – Wiley-VCH, Weinheim, Germany, 2009.
6. *Peggion C., Formaggio F., Crisma M., Epand R.F., Epand R.M., Toniolo C.* // J. Pept. Sci. – 2003. – **9**. – P. 679 – 689.
7. *Milov A.D., Tsvetkov Yu.D., Formaggio F., Crisma M., Toniolo C., Raap J.* // J. Amer. Chem. Soc. – 2000. – **122**. – P. 3843 – 3848.
8. *Milov A.D., Tsvetkov Yu.D., Raap J.* // Appl. Magn. Reson. – 2000. – **19**. – P. 215 – 226.
9. *Milov A.D., Tsvetkov Yu.D., Formaggio F., Crisma M., Toniolo C., Raap J.* // J. Amer. Chem. Soc. – 2001. – **123**. – P. 3784 – 3789.
10. *Milov A.D., Tsvetkov Yu.D., Formaggio F., Crisma M., Toniolo C., Millhauser G.L., Raap J.* // J. Phys. Chem. B. – 2001. – **105**. – P. 11206 – 11213.
11. *Milov A.D., Tsvetkov Yu.D., Formaggio F., Crisma M., Toniolo C., Raap J.* // J. Pept. Sci. – 2003. – **9**. – P. 690 – 700.
12. *Milov A.D., Tsvetkov Yu.D., Gorbunova E.Yu., Mustaeva L.G., Ovchinnikova T.V., Raap J.* // Biopolymers. – 2002. – **64**. – P. 328 – 336.
13. *Milov A.D., Tsvetkov Yu.D., Gorbunova E.Yu., Mustaeva L.G., Ovchinnikova T.V., Handgraaf J.-W., Raap J.* // Chem. Biodivers. – 2007. – **4**. – P. 1243 – 1255.
14. *Milov A.D., Samoilova R.I., Tsvetkov Yu.D., Peggion C., Formaggio F., Toniolo C., Raap J.* // Dokl. Rus. Acad. Sci.. – 2006. – **406**. – P. 341 – 345.
15. *Milov A.D., Samoilova R.I., Tsvetkov Yu.D., De Zotti M., Toniolo C., Raap J.* // J. Phys. Chem. B. – 2008. – **112**. – P. 13469 – 13472.
16. *Gobbo M., Poloni C., De Zotti M., Peggion C., Biondi B., Ballano G., Formaggio F., Toniolo C.* // Chem. Biol. Drug Des. – 2010. – **75**. – P. 169 – 181.
17. *De Zotti M., Biondi B., Peggion C., Park Y., Hahm K.-S., Formaggio F., Toniolo C.* // J. Pept. Sci. – 2011. – **17**. – P. 585-594.
18. *Toniolo C., Crisma M., Formaggio F., Peggion C.* // Biopolymers (Pept. Sci.) – 2001. – **60**. – P. 396 – 419.
19. *Gobbo M., Merli E., Biondi B., Oancea S., Toffoletti A., Formaggio F., Toniolo C.* // J. Pept. Sci. – 2012. – **18**. – P. 37 – 44.
20. *Milov A.D., Tsvetkov Yu.D., Maryasov A.G., Gobbo M., Prinzivalli C., De Zotti M., Formaggio F., Toniolo C.* // Appl. Magn. Res. – 2012. – **44**. – P. 495 – 508.
21. *Milov A.D., Salikhov K.M., Schirov M.D.* // Fiz. Tverd. Tela. (Leningrad). – 1981. – **23**. – P. 975 – 982.
22. *Pannier M., Veit S., Godt A., Jeschke G., Spiess H.W.* // J. Magn. Res. – 2000. – **142**. – P. 331 – 340.
23. *Larsen R.G., Singel D.J.* // J. Chem. Phys. – 1993. – **98**. – P. 5134 – 5146.
24. *Marko A., Margraf D., Cekan P., Sigurdsson S.T., Schiemann O., Prisner T.F.* // Phys. Rev. E. – 2010. – **81**. – P. 021911.
25. *Lovett J.E., Bowen A.M., Timmel C.R., Jones M.W., Dilworth J.R., Caprotti D., Bell S.G., Wong L.L., Harmer J.* // Phys. Chem. Chem. Phys. – 2009. – **11**. – P. 6840 – 6848.
26. *Marko A., Margraf D., Yu H., Mu Y., Stock G., Prisner T.* // J. Chem. Phys. – 2009. – **130**. – P. 064102.

27. *Schiemann O., Cekan P., Margraf D., Prisner T.F., Sigurdsson S.T.* // Angew. Chem. Int. Edit. – 2009. – **48**. – P. 3292 – 3295.
28. *Endeward B., Butterwick J.A., MacKinnon R., Prisner T.F.* // J. Amer. Chem. Soc. – 2009. – **131**. – P. 15246 – 15250.
29. *Milov A.D., Grishin Yu.A., Dzuba S.A., Tsvetkov Yu.D.* // Appl. Magn. Res. – 2011. – **41**. – P. 59 – 67.
30. *Milov A.D., Maryasov A.G., Tsvetkov Yu.D.* // Appl. Magn. Res. – 1998. – **15**. – P. 107 – 143.
31. *Kutsovsky Y.E., Mariasov A.G., Aristov Y.I., Parmon V.N.* // React. Kinet. Catal. Lett. – 1990. – **42**. – P. 19 – 24.
32. *Jeschke G., Koch A., Jones H., Godt A.* // J. Magn. Res. – 2002. – **155**. – P. 72 – 82.
33. *Godt A., Schulte M., Zimmermann H., Jeschke G.* // Angew. Chem. Int. Edit. – 2006. – **45**. – P. 7560 – 7564.
34. *Sicoli G., Mathis G., Aci-Seche S., Saint-Pierre C., Boulard Y., Gasparutto D., Gambarelli S.* // Nucl. Acids Res. – 2009. – **37**. – P. 3165 – 3176.
35. *Bode B.D., Margraf D., Plackmeyer J., Dürner G., Prisner T.F., Schiemann O.* // J. Amer. Chem. Soc. – 2007. – **129**. – P/ 6736 – 6744.
36. *Jeschke G., Sajid M., Schulte M., Godt A.* // Phys. Chem. Chem. Phys. – 2009. – **11**. – P. 6580 – 6591.
37. *Tikhonov A.N., Goncharsky A.V., Stepanov V.V., Yagoda A.G.* Numerical Methods for the Solution of Ill Posed Problems. – Kluwer Academic Publishers, Dordrecht, The Netherlands, 1995.
38. *Chiang Y.W., Borbat P.P., Freed J.H.* // J. Magn. Res. – 2005. – **172**. – P. 279 – 295.